$$B = \begin{bmatrix} 0.8153 & -0.0004 & 0.3234 & -0.0047 \\ -0.1595 & -0.0664 & -0.1655 & -0.8330 \\ 0 & 0 & 0.0028 & 0.0125 \\ 0 & 0 & 0 & 0 \\ 0 & 0 & 0.4118 & 1.8240 \end{bmatrix}$$

$$C = \begin{bmatrix} 1 & 0 & 0 & 0 & 0 \\ 0 & 1 & 0 & 0 & 0 \end{bmatrix}$$

Before applying any input-order reduction scheme, the inputs are normalized by scaling them by the inverse of their maximum values. The maximum values are given in the diagonal matrix S:

$$S = \text{diag}\{50, 10, 30, 15\}$$

Because the linear model is to be used for feedback control design, the reduced-order input is found by maximizing a Hankel norm.

A first-order reduced input is found in three iterations of Eqs. (9). The blending matrix scaled by S and reduced-order system Hankel norm are

$$S \cdot \boldsymbol{q}_1 = [43.51 \quad 0.2043 \quad 9.097 \quad 5.817]^T, \qquad J = 257362$$

Using the largest singular value approach described in the Introduction and used in Ref. 3 produces the following blending matrix, again scaled by S, and smaller Hankel norm:

$$S \cdot \boldsymbol{q}_{\text{sv}} = [-48.35 \quad -0.03424 \quad -7.391 \quad -0.9671]^T$$

$$J = 228080$$

To allow for control-variable decoupling, a second input direction is found. The scaled blending matrix and system Hankel norm are

$$S \cdot \boldsymbol{q}_2 = [22.01 \quad -0.4416 \quad -3.735 \quad -13.32]^T, \qquad J = 257802$$

For comparison, the full-input Hankel norm is 257,802. Note that the four scaled control input directions are, pairwise, 79.25, 50.52, 85.56, 72.66, 65.45, and 36.30 deg apart.

VII. Conclusions

A reduced-input system problem is formed with the objective of preserving system input–output properties. For exogenous inputs, a reduced-order input system $\mathcal{H}_\infty$ norm is maximized and an analytic solution is given. For control inputs, a reduced-order input system Hankel norm is maximized. Necessary conditions for the Hankel norm maximization are stated and an iterative solution is proposed. Although global convergence cannot be guaranteed, many practical applications have shown the achieved maxima to be very close to a known upper bound.

References

[1]Patton, R. J., and Chen, J., "Robust Fault Detection of Jet Engine Sensor Systems Using Eigenstructure Assignment," *Journal of Guidance, Control, and Dynamics*, Vol. 15, No. 6, 1992, pp. 1491–1497.

[2]Sobel, K. M., and Lallman, F. J., "Eigenstructure Assignment for the Control of Highly Augmented Aircraft," *Journal of Guidance, Control, and Dynamics*, Vol. 12, No. 3, 1989, pp. 1267–1276.

[3]Banda, S., and Bowlus, J., "Application of Multivariable Control Theory to Aircraft Control Laws," U.S. Air Force Research Lab., TR WL-TR-96-3099, May 1996.

[4]Doyle, J. C., Glover, K., Khargonekar, P. P., and Francis, B. A., "State-Space Solutions to Standard $\mathcal{H}_2$ and $\mathcal{H}_\infty$ Control Problems," *IEEE Transactions on Automatic Control*, Vol. AC-34, No. 8, 1989, pp. 831–847.

[5]Packard, A., and Doyle, J., "The Complex Structured Singular Value," Automatica, Vol. 29, No. 1, 1993, pp. 71–109.

[6]Zhou, K., Doyle, J. C., and Glover, K., *Robust and Optimal Control*, Prentice–Hall Upper Saddle River, NJ, 1996.

Nonlinear Modeling of Spacecraft Relative Motion in the Configuration Space

Pini Gurfil* and N. Jeremy Kasdin†
Princeton University, Princeton, New Jersey 08544

I. Introduction

THE analysis of relative spacecraft motion constitutes an issue of increasing interest. It was in the early 1960s that Clohessy and Wiltshire (CW) first published their celebrated work that utilized a Hill-like rotating coordinate system to derive expressions for the relative motion between satellites.[1] The CW linear formulation assumed small deviations from a circular reference orbit and used the initial conditions as the constants of motion. Since then, recognizing some of the limitations of this approach, others have generalized the CW equations for eccentric reference orbits[2] and to include perturbed dynamics.[3,4]

An important modification of the CW linear solution is the use of orbital elements as constants of motion instead of the Cartesian initial conditions. This concept, originally suggested by Hill,[5] has been widely used in the analysis of relative spacecraft motion.[3,6,7] Using this approach allows the examination of the effect of orbital perturbations on the relative motion via variational equations such as Lagrange's planetary equations (LPEs) or Gauss's variational equations (GVEs). Moreover, utilizing orbital elements facilitates the derivation of high-order, nonlinear extensions to the CW solution.

There have been a few reported efforts to obtain high-order solutions to the relative motion problem. Recently, Karlgaard and Lutze proposed formulating the relative motion in spherical coordinates in order to derive second-order expressions.[8] The use of Delaunay elements has also been proposed. For instance, Alfriend et al. derived differential equations in order to incorporate perturbations and high-order nonlinear effects into the modeling of relative dynamics.[9]

The present work establishes a methodology to obtain arbitrary high-order approximations to the relative motion between spacecraft by utilizing the Cartesian configuration space in conjunction with classical orbital elements. In other words, we propose utilizing the known inertial expressions describing vehicles flying in elliptic orbits in order to obtain, using a Taylor-series approximation, a time-series representation of the motion in a rotating frame, where the coefficients of the time series are functions of the orbital elements. We subsequently show that under certain conditions, this time series becomes a Fourier series. More important, in the process of the derivation, there is no need to solve differential equations. This significant merit results directly from utilization of the known inertial configuration space. The high-order approximation we present also provides important insights into boundedness of relative formation dynamics.

II. Problem Formulation

In the procedure to follow we study the relative motion of N vehicles (termed follower spacecraft) in arbitrary elliptic orbits relative to a circular reference orbit. We utilize the following standard coordinate systems: $\mathcal{I}$, a geocentric-equatorial inertial frame; $\mathcal{P}$, a

Received 16 September 2002; revision received 8 May 2003; accepted for publication 12 August 2003.

*Research Staff Member, Department of Mechanical and Aerospace Engineering; pgurfil@princeton.edu. Senior Member AIAA.

†Assistant Professor, Department of Mechanical and Aerospace Engineering; jkasdin@princeton.edu. Senior Member AIAA.

geocentric-perifocal coordinate system; and $\mathcal{L}$, an Euler–Hill coordinate system, rotating with mean motion n_{ref}. We assume that the reference orbit lies on the fundamental plane of the inertial reference system. The following treatment essentially provides a means for approximating relative motion between arbitrary (eccentric and inclined) Keplerian orbits. Due to the fact that the approximation is of high order (it can be truncated after a very large number of terms), the specific characteristics of the reference orbit (inclination, eccentricity) are of less importance than they are in the case of low-order approximations of relative motion.

The configuration space for the relative spacecraft dynamics in $\mathcal{L}$ is $\mathbb{R}^3$. Let $T_S(\mathbb{R}^3) = \mathbb{R}^3 \times \mathbb{R}^3$ be the tangent space of $\mathbb{R}^3$. We use $(\boldsymbol{r}, \dot{\boldsymbol{r}})$ as coordinates for $T_S(\mathbb{R}^3)$, namely, $(\boldsymbol{r}, \dot{\boldsymbol{r}}) \in T_S(\mathbb{R}^3)$. The differential equations of the spacecraft dynamics in the rotating frame $\mathcal{L}$ are (cf. Ref. 2)

$$\frac{\mathrm{d}}{\mathrm{d}t}\begin{bmatrix}\boldsymbol{r}\\ \dot{\boldsymbol{r}}\end{bmatrix}_{\mathcal{L}} = \begin{bmatrix}0_{3\times 3} & I_3\\ A_r & A_{\dot{r}}\end{bmatrix}\begin{bmatrix}\boldsymbol{r}\\ \dot{\boldsymbol{r}}\end{bmatrix}_{\mathcal{L}} + \begin{bmatrix}0\\ I_3\end{bmatrix}\left[\frac{\mu_E \boldsymbol{R}}{\|\boldsymbol{R}\|^3} - \frac{\mu_E(\boldsymbol{r}+\boldsymbol{R})}{\|\boldsymbol{r}+\boldsymbol{R}\|^3} + \boldsymbol{d} + \boldsymbol{u}\right]_{\mathcal{L}}, \qquad \boldsymbol{r}(t_0) = \boldsymbol{r}_0, \qquad \dot{\boldsymbol{r}}(t_0) = \dot{\boldsymbol{r}}_0 \tag{1}$$

where

$$A_r = \begin{bmatrix}n_{\text{ref}}^2 & 0 & 0\\ 0 & n_{\text{ref}}^2 & 0\\ 0 & 0 & 0\end{bmatrix}, \qquad A_{\dot{r}} = \begin{bmatrix}0 & 2n_{\text{ref}} & 0\\ -2n_{\text{ref}} & 0 & 0\\ 0 & 0 & 0\end{bmatrix} \tag{2}$$

and $\boldsymbol{R} = [R, 0, 0]^T$, R is the radius of the reference orbit, μ_E is the gravitational constant of the Earth, and $\boldsymbol{d} \in \mathbb{R}^3$ and $\boldsymbol{u} \in \mathbb{R}^3$ are perturbation and control vectors, respectively.

Approximate solutions for the configuration space over $\mathcal{L}$ can be obtained by linearization of Eq. (1) about the origin, assuming a circular reference orbit ($R = \text{const}$) and taking $\|\boldsymbol{r}\|/R$ to be first-order small. The resulting linear solution is most commonly parameterized as

$$\boldsymbol{r}(t, \boldsymbol{r}_0, \dot{\boldsymbol{r}}_0) = \tilde{\boldsymbol{\alpha}}_0(\boldsymbol{r}_0, \dot{\boldsymbol{r}}_0) + \tilde{\boldsymbol{\alpha}}_1^C(\boldsymbol{r}_0, \dot{\boldsymbol{r}}_0)\cos(n_{\text{ref}}t) + \tilde{\boldsymbol{\alpha}}_1^S(\boldsymbol{r}_0, \dot{\boldsymbol{r}}_0)\sin(n_{\text{ref}}t) + \tilde{\boldsymbol{r}}_d(t, \boldsymbol{r}_0, \dot{\boldsymbol{r}}_0) \tag{3}$$

where the constants $\tilde{\boldsymbol{\alpha}}_0 \triangleq [\tilde{\alpha}_0, \tilde{\beta}_0, \tilde{\gamma}_0]^T$, $\tilde{\boldsymbol{\alpha}}_k^C \triangleq [\tilde{\alpha}_k^C, \tilde{\beta}_k^C, \tilde{\gamma}_k^C]^T$, $\tilde{\boldsymbol{\alpha}}_k^S \triangleq [\tilde{\alpha}_k^S, \tilde{\beta}_k^S, \tilde{\gamma}_k^S]^T$ are functions of the initial position and velocity in $\mathcal{L}$, and $\tilde{\boldsymbol{r}}_d \in \mathbb{R}^3$ is a nonperiodic vector function.

For the unperturbed, uncontrolled case with a selection of initial conditions that yields $\tilde{\boldsymbol{r}}_d \equiv 0$, the periodic terms in Eq. (3) render a first-order Fourier series. Our objective here is to generalize this topology of the linearized solution, obtaining higher-order approximations via higher-order time-series expansions. To this end, we utilize classical orbital elements.[6,7] This idea also permits a straightforward and natural incorporation of orbital perturbations (via LPEs) and control forces (via GVEs).

To begin, let $\boldsymbol{\eta} = [a, e, i, \Omega, \omega, M_0]^T \in \mathbb{R}^2 \times \mathbb{S}^4$ be the classical osculating orbital elements, where a is the semimajor axis, e is the eccentricity, i is the inclination, Ω is the longitude of the ascending node, ω is the argument of the periapsis, and M_0 is the mean anomaly at epoch. Consider an osculating Keplerian elliptic orbit for a single vehicle in the formation (an extension to N vehicles is forthcoming) given by the conic equation

$$r = p/(1 + e\cos f) \tag{4}$$

where f is the true anomaly and $p = a(1 - e^2)$ is the semi–latus rectum. The position vector in the perifocal frame is thus given by

$$[\boldsymbol{r}]_{\mathcal{P}} = \begin{bmatrix}\dfrac{p}{1+e\cos f}\cos f\\ \dfrac{p}{1+e\cos f}\sin f\\ 0\end{bmatrix} \tag{5}$$

The transformation from the perifocal to the inertial frame is given by[10]

$$[\boldsymbol{r}]_{\mathcal{I}} = \begin{bmatrix}c(\Omega)c(\omega) - s(\Omega)s(\omega)c(i) & -c(\Omega)s(\omega) - s(\Omega)c(\omega)c(i) & s(\Omega)s(i)\\ s(\Omega)c(\omega) + c(\Omega)s(\omega)c(i) & -s(\Omega)s(\omega) + c(\Omega)c(\omega)c(i) & -c(\Omega)s(i)\\ s(\omega)s(i) & c(\omega)s(i) & c(i)\end{bmatrix}[\boldsymbol{r}]_{\mathcal{P}} \tag{6}$$

where, for the sake of conciseness, we used the usual notation $c(\cdot) \triangleq \cos(\cdot)$ and $s(\cdot) \triangleq \sin(\cdot)$. The transformation from the inertial frame $\mathcal{I}$ to the rotating, reference-orbit-centered frame $\mathcal{L}$ is written as

$$\boldsymbol{r} = \begin{bmatrix}\cos n_{\text{ref}}t & \sin n_{\text{ref}}t & 0\\ -\sin n_{\text{ref}}t & \cos n_{\text{ref}}t & 0\\ 0 & 0 & 1\end{bmatrix}[\boldsymbol{r}]_{\mathcal{I}} - \begin{bmatrix}R\\ 0\\ 0\end{bmatrix} \tag{7}$$

Substituting Eq. (5) into Eq. (6) and Eq. (6) into Eq. (7) yields the following expression for the position vector in the rotating frame:

$$\boldsymbol{r} = \frac{a(1-e^2)}{1+e\cos f}\begin{bmatrix}\cos(f+\omega)\cos(n_{\text{ref}}t - \Omega) + \cos i\sin(f+\omega)\sin(n_{\text{ref}}t - \Omega) - R\\ \cos i\cos(n_{\text{ref}}t - \Omega)\sin(f+\omega) - \cos(f+\omega)\sin(n_{\text{ref}}t - \Omega)\\ \sin i\sin(f+\omega)\end{bmatrix} \tag{8}$$

Eq. (8) provides the general nonlinear expression for the relative position vector as a function of (possibly osculating) orbital elements and time in a rotating frame of reference centered on a circular, equatorial orbit. Although Eq. (8) may be used to investigate the relative dynamics of a spacecraft formation, it has three main drawbacks: it provides very little insight into the relative motion dynamics, it is highly nonlinear, and the time dependence is implicit due to the f-dependent terms. It is thus desirable to expand Eq. (8) into a time series of the following form:

$$\boldsymbol{r}(t, \boldsymbol{\eta}) = \boldsymbol{\alpha}_0(\boldsymbol{\eta}) + \sum_{k=1}^{\infty}\left[\boldsymbol{\alpha}_k^C(\boldsymbol{\eta})\cos(kn_{\text{ref}}t) + \boldsymbol{\alpha}_k^S(\boldsymbol{\eta})\sin(kn_{\text{ref}}t)\right] + \boldsymbol{r}_d(t, \boldsymbol{\eta}) \tag{9}$$

where $\boldsymbol{\alpha}_0 \triangleq [\alpha_0, \beta_0, \gamma_0]^T$, $\boldsymbol{\alpha}_k^C \triangleq [\alpha_k^C, \beta_k^C, \gamma_k^C]^T$, $\boldsymbol{\alpha}_k^S \triangleq [\alpha_k^S, \beta_k^S, \gamma_k^S]^T$ are functions of the (possibly osculating) orbital elements. Eq. (9) constitutes an orbital-elements-based generalization of the first-order Cartesian parameterization (3). It is shown in Sec. III, using a mapping from true anomaly to time via the mean anomaly, that Eq. (8) can indeed be represented in the form of Eq. (9).

For a formation of N vehicles (in addition to the actual or virtual leader), the relative position vector of vehicle q relative to vehicle j is therefore given by

$$\boldsymbol{r}_{qj}(t, \boldsymbol{\eta}_q, \boldsymbol{\eta}_j) = \boldsymbol{\alpha}_0(\boldsymbol{\eta}_q, \boldsymbol{\eta}_j) + \sum_{k=1}^{\infty}\left\{\boldsymbol{\alpha}_k^C(\boldsymbol{\eta}_q, \boldsymbol{\eta}_j)\cos(kn_{\text{ref}}t) + \boldsymbol{\alpha}_k^S(\boldsymbol{\eta}_q, \boldsymbol{\eta}_j)\sin(kn_{\text{ref}}t)\right\} + \boldsymbol{r}_d(t, \boldsymbol{\eta}_q, \boldsymbol{\eta}_j) \tag{10}$$

where $\boldsymbol{r}_{qj}(t,\boldsymbol{\eta}_q,\boldsymbol{\eta}_j) \triangleq \boldsymbol{r}(t,\boldsymbol{\eta}_q) - \boldsymbol{r}(t,\boldsymbol{\eta}_j)$, $\boldsymbol{\alpha}_0(\boldsymbol{\eta}_q,\boldsymbol{\eta}_j) \triangleq \boldsymbol{\alpha}_0(\boldsymbol{\eta}_q) - \boldsymbol{\alpha}_0(\boldsymbol{\eta}_j)$, $\boldsymbol{\alpha}_k^C(\boldsymbol{\eta}_q,\boldsymbol{\eta}_j) \triangleq \boldsymbol{\alpha}_k^C(\boldsymbol{\eta}_q) - \boldsymbol{\alpha}_k^C(\boldsymbol{\eta}_j)$, and $\boldsymbol{\alpha}_k^S(\boldsymbol{\eta}_q,\boldsymbol{\eta}_j) \triangleq \boldsymbol{\alpha}_k^S(\boldsymbol{\eta}_q) - \boldsymbol{\alpha}_k^S(\boldsymbol{\eta}_j)$. By truncating the series in Eqs. (9) or (10) at order m, we have an mth-order approximation to the relative motion.

III. High-Order Closed-Form Approximations

For a circular, equatorial reference orbit, the orbital elements Ω and ω are undefined. We therefore use instead the degenerate set of orbital elements $\tilde{\boldsymbol{\eta}} = [a, e, i, \varepsilon]^T$ where $\varepsilon = \Omega + \omega - M_0$ is the mean longitude at epoch. In the derivation to follow, we utilize the normalization $R = \mu_E = n_{\text{ref}} = 1$, resulting in the normalized reference orbital elements $\tilde{\boldsymbol{\eta}}_{\text{ref}} = [1, 0, 0, 0]^T$. The degenerate set of orbital elements for an arbitrary follower spacecraft in the formation is thus given by $\tilde{\boldsymbol{\eta}} = \tilde{\boldsymbol{\eta}}_{\text{ref}} + \delta\boldsymbol{\eta}$ with $\delta\boldsymbol{\eta} = [\delta a, e, i, \varepsilon]^T$. The analysis is completed by expanding Eq. (8) into a Taylor series about $\boldsymbol{\eta}_{\text{ref}}$ in powers of $\delta\boldsymbol{\eta}$.

However, to obtain a time-series expansion of the form of Eq. (9), we must first relate true anomaly to time. This is performed by introducing the mean anomaly M and using the following series solution to Kepler's equation[10]:

$$f = M + 2\sum_{l=1}^{\infty}\frac{1}{l}\left[\sum_{s=-\infty}^{\infty} J_s(-le)\left(\frac{1-\sqrt{1-e^2}}{e}\right)^{|l+s|}\right]\sin(lM) \tag{11}$$

where $J_s(\cdot)$ is a Bessel function of the first kind of order s. For illustration, for terms up to order e^2, Eq. (11) can be expanded as[10]

$$f = M + 2e\sin(M) + 5/4e^2\sin(2M) + \mathcal{O}(e^3) \tag{12}$$

Substituting $M \triangleq t/(1+\delta a)^{3/2} - M_0$ into Eq. (11) yields the desired mapping $f(t) : t \to f$, which is then substituted into Eq. (8). The time-series expansion (9) is now available by writing the multivariable Taylor series

$$\begin{aligned}\boldsymbol{r}(t,\tilde{\boldsymbol{\eta}}) = \boldsymbol{r}(t,\boldsymbol{\eta}) &= \boldsymbol{r}(\tilde{\boldsymbol{\eta}}_{\text{ref}}) + \sum_{l=1}^{\infty}\left[\frac{1}{l!}(\delta\boldsymbol{\eta}\cdot\nabla_{\tilde{\eta}})^l\boldsymbol{r}(t,\tilde{\boldsymbol{\eta}})\right]_{\tilde{\eta}=\tilde{\boldsymbol{\eta}}_{\text{ref}}}\\ &= \boldsymbol{\alpha}_0(\boldsymbol{\eta}) + \sum_{k=1}^{\infty}\left[\boldsymbol{\alpha}_k^C(\boldsymbol{\eta})\cos(kt) + \boldsymbol{\alpha}_k^S(\boldsymbol{\eta})\sin(kt)\right] + \boldsymbol{r}_d(t,\boldsymbol{\eta})\end{aligned} \tag{13}$$

Based on Eq. (13), expressions for the relative motion between follower spacecraft are easily obtained. In the next section, we illustrate this methodology using second-order expansions.

IV. Example: Second-Order Solutions

Truncated to include the zero-, first- and second-order terms only, and utilizing the identity $(\delta\boldsymbol{\eta}\cdot\nabla_{\tilde{\eta}})(\delta\boldsymbol{\eta}\cdot\nabla_{\tilde{\eta}})\boldsymbol{r}(t,\tilde{\boldsymbol{\eta}}) = \delta\boldsymbol{\eta}\cdot\nabla_{\tilde{\eta}}[\delta\boldsymbol{\eta}\cdot\nabla_{\tilde{\eta}}(\boldsymbol{r}(t,\tilde{\boldsymbol{\eta}}))] = \delta\boldsymbol{\eta}\cdot[\delta\boldsymbol{\eta}\cdot\nabla_{\tilde{\eta}}(\nabla_{\tilde{\eta}}\boldsymbol{r}(t,\tilde{\boldsymbol{\eta}}))]$, Eq. (13) becomes

$$\begin{aligned}\boldsymbol{r}(t,\boldsymbol{\eta}) \approx{}& \boldsymbol{r}(\tilde{\boldsymbol{\eta}}_{\text{ref}}) + (\delta\boldsymbol{\eta}\cdot\nabla_{\tilde{\eta}})\boldsymbol{r}(t,\tilde{\boldsymbol{\eta}})|_{\tilde{\eta}=\tilde{\eta}_{\text{ref}}}\\ &+ \tfrac{1}{2}\delta\boldsymbol{\eta}\cdot[\delta\boldsymbol{\eta}\cdot\nabla_{\tilde{\eta}}(\nabla_{\tilde{\eta}}\boldsymbol{r}(t,\tilde{\boldsymbol{\eta}}))]|_{\tilde{\eta}=\tilde{\eta}_{\text{ref}}}\end{aligned} \tag{14}$$

Performing the symbolic calculation in Eq. (14), simplifying, and rewriting into the time series (9) yields

$$\boldsymbol{r}(t,\boldsymbol{\eta}) \approx \boldsymbol{\alpha}_0(\boldsymbol{\eta}) + \sum_{k=1}^{2}\left[\boldsymbol{\alpha}_k^C(\boldsymbol{\eta})\cos(kt) + \boldsymbol{\alpha}_k^S(\boldsymbol{\eta})\sin(kt)\right] + \boldsymbol{r}_d(t,\boldsymbol{\eta}) \tag{15}$$

where

$$\boldsymbol{\alpha}_0 = \begin{bmatrix}\delta a - \frac{1}{2}\varepsilon^2 - \frac{1}{4}i^2 - \frac{1}{2}e^2\\ \varepsilon(1+\delta a)\\ -\frac{3}{2}ie\sin(\omega)\end{bmatrix} \tag{16}$$

$$\boldsymbol{\alpha}_1^C = \begin{bmatrix}2\varepsilon e\sin(M_0) - (1+\delta a)e\cos(M_0)\\ -2(1+\delta a)e\sin(M_0) - \varepsilon e\cos(M_0)\\ i(1+\delta a)\sin(\omega - M_0)\end{bmatrix}$$

$$\boldsymbol{\alpha}_1^S = \begin{bmatrix}-(1+\delta a)e\sin(M_0) - 2\varepsilon e\cos(M_0)\\ 2(1+\delta a)e\cos(M_0) + \varepsilon e\sin(M_0)\\ i(1+\delta a)\cos(\omega - M_0)\end{bmatrix} \tag{17}$$

$$\boldsymbol{\alpha}_2^C = \begin{bmatrix}\frac{1}{4}i^2\cos[2(\omega - M_0)] + \frac{1}{2}e^2\cos(2M_0)\\ -\frac{1}{4}i^2\sin[2(\omega - M_0)] - \frac{1}{4}e^2\sin(2M_0)\\ \frac{1}{2}ie\sin(\omega - 2M_0)\end{bmatrix}$$

$$\boldsymbol{\alpha}_2^S = \begin{bmatrix}-\frac{1}{4}i^2\sin[2(\omega - M_0)] + \frac{1}{2}e^2\sin(2M_0)\\ -\frac{1}{4}i^2\cos[2(\omega - M_0)] + \frac{1}{4}e^2\cos(2M_0)\\ \frac{1}{2}ie\cos(\omega - 2M_0)\end{bmatrix} \tag{18}$$

The nonperiodic terms are given by

$$\boldsymbol{r}_d = \begin{bmatrix}\frac{3}{2}\varepsilon\delta at + \frac{3}{2}e\delta at\sin(t - M_0) - \frac{9}{8}\delta a^2t^2\\ -\frac{3}{2}\delta at + \frac{3}{2}e\delta at\cos(t - M_0) + \frac{3}{8}\delta a^2t\\ -\frac{3}{2}i\delta at\cos(t + \omega - M_0)\end{bmatrix} \tag{19}$$

Note that since $\boldsymbol{\alpha}_0 \neq 0$, the center of motion of a follower spacecraft in the rotating frame is offset relative to the reference orbit.

Important results regarding the boundedness of relative motion are obtained by examining the terms in $\boldsymbol{r}_d$. First, note the second-order secular drift in the normal direction for $\delta a \neq 0$. This phenomenon is not predicted by the CW approximation. It stems from the converging–diverging nature of the time series approximating the relative motion; if an infinite number of terms is taken in the approximation, we see convergence to the exact expression for the relative position vector in Eq. (8), which is of course bounded if the spacecraft follows an elliptic Keplerian orbit (and periodic, if the orbital rates are commensurate). Also, note that bounded (nonosculating) motion is obtained if and only if $\delta a_q = \delta a_j$.

To illustrate the utility of the second-order approximation, we have simulated the motion of a follower spacecraft with $a = 200$ km, $\delta a = 0$, $e = 0.02$, $i = 15$ deg, $\Omega = 5$ deg, and $\omega = M_0 = 0$. Figure 1 depicts a comparison of the exact, nonlinear solution of Eq. (8), the second-order approximation of Eqs. (15–19), and the CW linear approximation. Notably, the second-order approximation fits considerably better to the exact solution due to the obvious

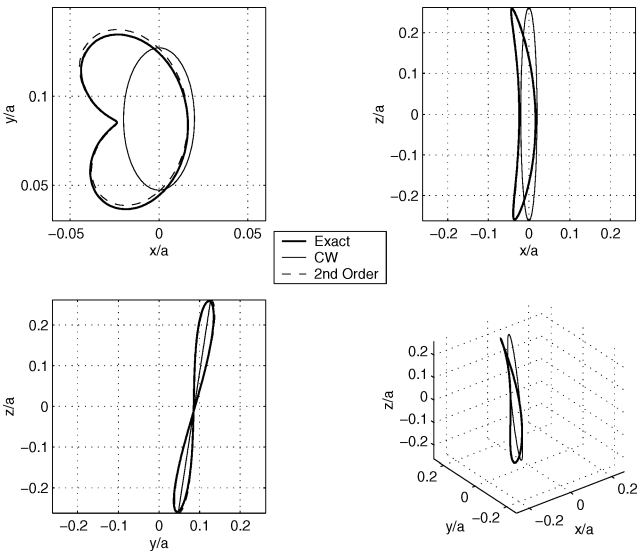

Fig. 1 Motion of a follower spacecraft in the reference-orbit-centered rotating frame: comparison of exact, CW, and second-order approximations.

limitation of the CW approximation to small relative inclinations and eccentricities.

V. Conclusions

This paper presented a framework for approximating the relative dynamics of spacecraft formations utilizing the known three-dimensional inertial solutions. Based on the results, we may conclude that the time-series parameterization of the relative position vector lends itself naturally to high orders and, hence, constitutes a powerful analysis and modeling tool, providing much insight into the relative dynamics of spacecraft formations. The insight obtained from the nonlinear modeling may be used to design "natural" orbits for formation flying, thus further reducing fuel consumption.

Based on the first illustrative example, we further conclude that second-order solutions are sufficient to adequately approximate orbits having high relative inclinations and eccentricities, where the CW approximation fails.

References

[1]Clohessy, W. H., and Wiltshire, R. S., "Terminal Guidance System for Satellite Rendezvous," *Journal of Astronautical Sciences*, Vol. 27, No. 9, 1960, pp. 653–678.

[2]Inalhan, G., Tillerson, M., and How, J. P., "Relative Dynamics and Control of Spacecraft Formations in Eccentric Orbits," *Journal of Guidance, Control, and Dynamics*, Vol. 25, No. 1, 2002, pp. 48–60.

[3]Gim, D. W., and Alfriend, K. T., "The State Transition Matrix of Relative Motion for the Perturbed Non-Circular Reference Orbit," American Astronomical Society, Paper AAS 01-222, Washington, D.C., Feb. 2001.

[4]Alfriend, K. T., and Schaub, H., "Dynamics and Control of Spacecraft Formations: Challenges and Some Solutions," *Journal of Astronautical Sciences*, Vol. 48, No. 2, 2000, pp. 249–267.

[5]Hill, G. W., "Researches in the Lunar Theory," *American Journal of Mathematics*, Vol. 1, 1878, pp. 5–26.

[6]Schaub, H., Vadali, S. R., and Alfriend, K. T., "Spacecraft Formation Flying Control Using Mean Orbital Elements," *Journal of Astronautical Sciences*, Vol. 48, No. 1, 2000, pp. 69–87.

[7]Schaub, H., and Alfriend, K., "Hybrid Cartesian and Orbit Elements Feedback Law for Formation Flying Spacecraft," *Journal of Guidance, Control, and Dynamics*, Vol. 25, No. 2, 2002, pp. 387–393.

[8]Karlgaard, C. D., and Lutze, F. H., "Second-Order Relative Motion Equations," American Astronomical Society, Paper AAS 01-464, Washington, D.C., July 2001.

[9]Alfriend, K. T., Yan, H., and Vadali, S. R., "Nonlinear Considerations in Satellite Formation Flying," AIAA Paper 2002-4741, Aug. 2002.

[10]Battin, R. H., *An Introduction to the Mathematics and Methods of Astrodynamics*, AIAA, Reston, VA, 1999, Chap. 10, pp. 485–488.